Available online at www.sciencedirect.com
SCIENCE DIRECT®
International Journal of Thermal Sciences 44 (2005) 766–773
International Journal of Thermal Sciences
www.elsevier.com/locate/ijts

Scalar transport modelling in turbulent round jets with co-flowing stream

Mohamed Hichem Gazzah [a,*], Hafedh Belmabrouk [a], Mohamed Sassi [b]

[a] *Département de physique, faculté des sciences de Monastir, avenue de l'environnement 5019 Monastir, Tunisia*
[b] *Département de mécanique, école nationale d'ingénieurs de Tunis, BP 37, 1002 Belvédère Tunis, Tunisia*

Received 30 January 2004; received in revised form 4 January 2005; accepted 24 January 2005

Available online 29 March 2005

Abstract

In this numerical study, several traditional scalar dissipation rate models are used for scalar transport modelling in mixing turbulent round jets with co-flowing air. These models are implemented into a second order turbulence closure model and are compared to the published experimental data. It is shown that the assumption of equal time scales for dynamic and scalar turbulence is no longer needed when the algebraic non-equal scales model or the transport equation model are used. The influence of these models on scalar mixture fraction, unmixedness, half-width of the jet and time scale ratio are examined. It is shown that the trends, which are observed in the experiments, are reproduced qualitatively by the non-equal scales model.

Keywords: Jet; Turbulent; Co-flow; Scalar; Models

1. Introduction

Turbulent jets with co-flowing air have attracted considerable attention (Borean et al. [1], Antoine et al. [2], Schefer and Dibble [3], Gazzah et al. [4]), in the aim of increasing the efficiency of mixing processes in industrial applications, such as turbulent diffusion flames in combustion chambers and aeronautics. However, a major difficulty in the modeling of turbulent flames is the adequate modeling of scalar turbulence.

To investigate turbulent binary-mixing jets numerically, one has to use an algebraic equation or a transport equation for the scalar dissipation rate ε_f. Several models have been used in the literature and some examples have been cited by Schiestel [5] and Ruffin [6]. The k–ε or second order models based on the assumption of equal velocity and scalar scales have been tested. However, this assumption disagrees with the experimental data obtained in turbulent jets and turbulent diffusion flames. Indeed, the measured ratio of the mechanical to scalar time scale in the helium-air jet of Panchapakesan and Lumley [7] was not constant. Dibble et al. [8] calculated the time scale ratio in a turbulent diffusion flame using a second-order closure model and found out that the ratio is not constant. Lucas [9] and Pietri et al. [10] found a varying mechanical to scalar time scale ratio in their experiment on axisymmetric jet.

A transport equation for the scalar dissipation rate must be constructed to overcome the assumption of equal time scales for the scalar and the velocity turbulence. In this purpose, Shih et al. [11], Mantel and Borghi [12], Ruffin [6] developed some equations for the scalar dissipation rate in the frame of second order closures. However, Yoshizawa [13] developed an algebraic model for ε_f with his two-scale direct interaction approximation (TSDIA), which does not rely on the assumption of equal length and time scales for dynamic and scalar turbulence. This model is called the non-equal scales model for scalar transport.

In the present study, we investigate a turbulent binary-mixing round jet of propane emerging at high velocity from a nozzle into a co-flowing air. The algebraic equal scales model, the non-equal scales model of Yoshizawa [13] and the transport equation model of Mantel and Borghi [12] are

* Corresponding author. Tel.: +216 73 500 274; fax: +216 73 500 278.
E-mail address: hichem.gazzah@fsm.rnu.tn (M.H. Gazzah).

1290-0729/$ – see front matter
doi:10.1016/j.ijthermalsci.2005.01.007

Nomenclature

D	nozzle diameter	m
D_e	effective diameter	m
D_F	diffusion coefficient	$m^2 \cdot s^{-1}$
$\widetilde{F}$	mean mixture fraction	
L_f	scalar halfwidth	
k	turbulent kinetic energy	$m^2 \cdot s^{-2}$
K_f	scalar decay constant	
R_τ	time scale ratio	
r	radial distance	m
$\widetilde{U}$	mean axial velocity	$m \cdot s^{-1}$
$\widetilde{V}$	mean radial velocity	$m \cdot s^{-1}$
u	axial velocity	$m \cdot s^{-1}$
v	radial velocity	$m \cdot s^{-1}$
w	tangential velocity	$m \cdot s^{-1}$
x	axial distance	m
g, $\tilde{f}''^2$	scalar variance	
Re	Reynolds number	
Re_t	turbulent Reynolds number	
S_ρ	density ratio, $= \rho_j/\rho_{co}$	
Sc_t	turbulent Schmidt number	
$S_f^{1/2}$	spreading rate	

Greek symbols

β_e	expansion coefficient	
μ	dynamic viscosity	$kg \cdot m^{-1} \cdot s^{-1}$
ν	kinematic viscosity	$m^2 \cdot s^{-1}$
ε	dissipation rate	$m^2 \cdot s^{-3}$
ε_f	scalar dissipation rate	s^{-1}
ρ	density	$kg \cdot m^{-3}$
Φ	generalized turbulent parameter	

Subscripts

ex	external
a	ambient fluid
c	centerline
co	coflow
max	maximum
j	jet fluid

applied within a second order turbulence closure model. The influence of the co-flow on the various physical quantities of the propane/air jet are analyzed using these last models and compared to the experimental data of Schefer and Dibble [3].

2. Velocity and scalar turbulence modeling

2.1. Velocity turbulence modeling

The turbulent flow is modeled using Favre averaged quantities. The second order turbulence closure model is used to describe the turbulent velocity field. The parabolized equations and the constants of this model are reported, for example, in Sanders et al. [14].

A mass weighted quantity is defined as

$$\widetilde{\Phi} = \frac{\overline{\rho\Phi}}{\bar{\rho}} \tag{1}$$

This Favre-averaged variable is denoted by a tilde $\widetilde{\Phi}$, while a conventional averaged variable is denoted by an overbar $\overline{\Phi}$. Favre fluctuations are denoted by Φ'', while conventional fluctuations are indicated by Φ'. The resulting governing equations in cylindrical coordinates are developed using the standard parabolic flow assumption. The continuity equation is given by

$$\frac{\partial \bar{\rho}\widetilde{U}}{\partial x} + \frac{1}{r}\frac{\partial (r\bar{\rho}\widetilde{V})}{\partial r} = 0 \tag{2}$$

where x is the axial distance in the jet direction and r is the radial distance. The equation for axial momentum is

$$\frac{\partial \bar{\rho}\widetilde{U}\widetilde{U}}{\partial x} + \frac{1}{r}\frac{\partial r\bar{\rho}\widetilde{V}\widetilde{U}}{\partial r} = -\frac{\partial \overline{P}}{\partial x} + \frac{1}{r}\frac{\partial}{\partial r}\left(r\mu\frac{\partial \widetilde{U}}{\partial r}\right) - \frac{1}{r}\frac{\partial (r\overline{\rho v'' u''})}{\partial r} + \bar{\rho} g \tag{3}$$

when $\partial \overline{P}/\partial x \approx \rho_a g$ a buoyancy term is often introduced and written as $-(\rho_a - \bar{\rho})g$. However, buoyancy effects are omitted in the present study, and the mean pressure gradient is assumed zero.

To describe the mixing of gases, a mixture fraction $\widetilde{F}$, is introduced. It is governed by a convection-diffusion conservation equation of the form

$$\frac{\partial \bar{\rho}\widetilde{U}\widetilde{F}}{\partial x} + \frac{1}{r}\frac{\partial r\bar{\rho}\widetilde{V}\widetilde{F}}{\partial r} = +\frac{1}{r}\frac{\partial}{\partial r}\left(r\rho D_F\frac{\partial \widetilde{F}}{\partial r}\right) - \frac{1}{r}\frac{\partial (r\overline{\rho v'' f''})}{\partial r} \tag{4}$$

The mean density can be obtained from the mean mixture fraction using the equation of state, which with constant pressure, leads to

$$\frac{1}{\bar{\rho}} = \frac{\widetilde{F}}{\rho_j} + \frac{1-\widetilde{F}}{\rho_a} \tag{5}$$

where ρ_a is the ambient air density and ρ_j is the nozzle fluid density.

The equation of state can also be written as

$$\bar{\rho} = \bar{\rho} a \widetilde{F} + b \tag{6}$$

where a and b are two constants based only on the mass density of specie in their pure states ($a = (\rho_j - \rho_a)/\rho_j$ and $b = \rho_a$).

The turbulent flow is modeled using Favre averaged quantities. A second order turbulence model is used to describe

Table 1
Source terms in the general equation (7) for the second order model. Here $G=-\bar{\rho}\beta_e g\widetilde{u''f''}$ is the buoyancy production term and $P=-\bar{\rho}\widetilde{u''v''}\frac{\partial\tilde{U}}{\partial r}$ is the production term of turbulent energy

Φ	S_Φ
$\widetilde{u''u''}$	$-2(1-\alpha)\bar{\rho}\widetilde{u''v''}\frac{\partial\tilde{U}}{\partial r}-\frac{2}{3}\bar{\rho}\varepsilon-C_1\bar{\rho}\frac{\varepsilon}{k}\left(\widetilde{u''u''}-\frac{2}{3}k\right)+\frac{2}{3}\alpha P-\left(2-\frac{4}{3}C_3\right)\bar{\rho}\beta_e g_x\widetilde{u''f''}$
$\widetilde{v''v''}$	$-\frac{2}{3}\bar{\rho}\varepsilon-C_1\bar{\rho}\frac{\varepsilon}{k}\left(\widetilde{v''v''}-\frac{2}{3}k\right)+\frac{2}{3}\alpha P-\frac{2C_s}{r^2}\frac{k}{\varepsilon}\bar{\rho}\widetilde{w''w''}\left(\widetilde{v''v''}-\widetilde{w''w''}\right)-\frac{2}{3}C_3\bar{\rho}\beta_e g_x\widetilde{u''f''}$
$\widetilde{w''w''}$	$-\frac{2}{3}\bar{\rho}\varepsilon-C_1\bar{\rho}\frac{\varepsilon}{k}\left(\widetilde{w''w''}-\frac{2}{3}k\right)+\frac{2}{3}\alpha P+\frac{2C_s}{r^2}\frac{k}{\varepsilon}\bar{\rho}\widetilde{w''w''}\left(\widetilde{v''v''}-\widetilde{w''w''}\right)-\frac{2}{3}C_3\bar{\rho}\beta_e g_x\widetilde{u''f''}$
$\widetilde{u''v''}$	$-(1-\alpha)\bar{\rho}\widetilde{v''v''}\frac{\partial\tilde{U}}{\partial r}-C_1\bar{\rho}\frac{\varepsilon}{k}\widetilde{u''v''}-\frac{C_s}{r^2}\frac{k}{\varepsilon}\bar{\rho}\widetilde{w''w''}\widetilde{u''v''}-(1-C_3)\bar{\rho}\beta_e g_x\widetilde{u''f''}$
ε	$\frac{k}{\varepsilon}\left(C_{\varepsilon,1}(P+G)-C_{\varepsilon,2}\bar{\rho}\varepsilon\right)$
$\widetilde{u''f''}$	$-\bar{\rho}\widetilde{v''f''}\frac{\partial\tilde{U}}{\partial r}-\bar{\rho}\widetilde{u''v''}\frac{\partial\tilde{F}}{\partial r}-C_{1f}\bar{\rho}\frac{\varepsilon}{k}\widetilde{u''f''}-C'_{1f}\bar{\rho}\frac{\varepsilon}{k}\left(\frac{\widetilde{u''u''}}{2k}\widetilde{u''f''}+\left(\frac{\widetilde{u''v''}}{2k}-\frac{1}{3}\right)\widetilde{v''f''}\right)$ $+0.8\bar{\rho}\widetilde{v''f''}\frac{\partial\tilde{U}}{\partial r}-(1-C_{3f})\bar{\rho}\beta_e g_x\widetilde{f''^2}$
$\widetilde{v''f''}$	$-\bar{\rho}\widetilde{v''f''}\frac{\partial\tilde{V}}{\partial r}-\bar{\rho}\widetilde{v''v''}\frac{\partial\tilde{F}}{\partial r}-C_{sf}\bar{\rho}\frac{k}{\varepsilon}\frac{\widetilde{w''w''}}{r^2}\widetilde{v''f''}-C_{1f}\bar{\rho}\frac{\varepsilon}{k}\widetilde{v''f''}$ $-C'_{1f}\bar{\rho}\frac{\varepsilon}{k}\left(\frac{\widetilde{u''v''}}{2k}\widetilde{u''f''}+\left(\frac{\widetilde{v''v''}}{2k}-\frac{1}{3}\right)\widetilde{v''f''}\right)-0.2\bar{\rho}\widetilde{u''f''}\frac{\partial\tilde{U}}{\partial r}$
$\tilde{f''^2}=g$	$-2\bar{\rho}\widetilde{v''f''}\frac{\partial\tilde{F}}{\partial r}-\bar{\rho}\varepsilon_f$

the velocity turbulent field. The equations and constants of this model are reported in Sanders et al. [14]. The parabolized conservation equations in cylindrical coordinates may be presented in the following general form:

$$\frac{\partial\bar{\rho}\tilde{U}\Phi}{\partial x}+\frac{1}{r}\frac{\partial(r\bar{\rho}\tilde{V}\Phi)}{\partial r}=\frac{1}{r}\frac{\partial}{\partial r}\left(r\bar{\rho}D_\Phi\frac{\partial\Phi}{\partial r}\right)+S_\Phi \qquad (7)$$

where Φ is the dependent variable, D_Φ is the diffusion coefficient of the property Φ, and S_Φ is the source term of Φ. The relevant variables and the associated transport coefficients and source terms are shown in Table 1.

In the literature a number of modifications to the ε-equation model have been proposed to correct the spreading rate for the round jet, but many attempts have failed because it proved to deteriorate predictions for other types of flow. In fact, the standard version of ε-equation model is due to Launder and Spalding [15]. Their model constants are calibrated for the incompressible case by comparison to experimental results of a wall jet and a mixing layer. When the flow is complicated, modified versions of the ε-equation model were proposed to take into account these effects. The same approach was adopted when density variations were caused by mixing. The modifications introduced to the ε transport equations, in these cases, are often by addition of supplementary terms. Pope [16] suggested to add a term to the ε-equation based on the idea of vortex stretching, which would only be active in the round jet. However with this term the spreading rate of a radial jet is underpredicted by 60% (Rubel [17]). Furthermore the resulting model does not comply with realizability which is one of the constraints which can be imposed on turbulence models (Speziale [18]). Other researchers modified the dissipation rate equation by changing to the model constants (Borghi and Escudie [19], Sanders et al. [14]).

To improve the predictions of the round jet spreading rate, the turbulent exchange of momentum must be diminished and consequently the eddy-viscosity must be decreased. This is often done by changing this empirical coefficients $C_{\varepsilon,1}$ and $C_{\varepsilon,2}$ in the ε-equation. In our case, the ε-equation model constants were adjusted by the correct prediction of the jet expansion. The used constants are summarised in Table 2.

Table 2
Turbulence constants in the second order model, where the value of C_1 is adapted for the axisymmetric jet case [14]. The diffusion coefficient is defined by $D_\Phi=C_\Phi\frac{k}{\varepsilon}\widetilde{v''v''}$. For all Reynolds stresses $C_\Phi=C_s$, while for the scalar fluxes and the scalar variance $C_\Phi=C_{sf}$

C_1	α	C_3	C_s	$C_{\varepsilon,1}$	$C_{\varepsilon,2}$	$C_{1,f}$	$C'_{1,f}$	$C_{3,f}$	$C_{s,f}$
2.3	0.6	0.5	0.22	1.45	1.90	5.7	−6.1	0.33	0.22

The second order closure model consists of non-isotropic expressions for the Reynolds stresses and turbulent scalar fluxes. The transport equations for the Reynolds stresses, the variance of the mixture fraction, the scalar fluxes, the turbulent kinetic energy and the scalar dissipation rates are developed using the parabolic flow assumption. The model constants used in the present study are given in Table 2.

2.2. Algebraic equal-scales model of the scalar dissipation rate model

The classical algebraic equal-scales of the scalar dissipation rate ε_f is based on the assumption that the time and length scales of velocity and scalar turbulent fields are equal. The time and length scales for velocity turbulence are $\tau_u\sim k/\varepsilon$ and $l_u\sim k^{3/2}/\varepsilon$, respectively, where k is the turbulent kinetic energy and ε is its dissipation rate. On the basis of dimensional analysis, the time and length scales for scalar turbulence are $\tau_s\sim g/\varepsilon_f$ and $l_s\sim g^{3/2}\varepsilon^{1/2}/\varepsilon_f^{3/2}$, respectively, where g is the scalar variance. Setting $\tau_u=\tau_s$ or $l_u=l_s$ gives the equal-scales model:

$$\varepsilon_f=R_\tau\varepsilon g/k \qquad (8)$$

where the coefficient R_τ is empirical and it is usually taken to be equal to 2 (Schiestel [5]).

The assumption of equal length scales leads to a fixed turbulent Schmidt number. The turbulent Schmidt number, Sc_t, is defined as the ratio of the eddy viscosity $\nu_t \sim k^2/\varepsilon$ and the eddy diffusivity $\nu_s \sim g^2\varepsilon/\varepsilon_f^2$. This expression leads to a relationship between Sc_t and R_τ which is obtained from $Sc_t = \nu_t/\nu_s \sim (k^2/\varepsilon)/(g^2\varepsilon/\varepsilon_f^2)$, so that $Sc_t \sim R_\tau^2$.

2.3. Yoshizawa non-equal-scale of the scalar dissipation rate model

To overcome the shortcoming of the previous model, Yoshizawa [13] has developed a model based on the two-scale direct interaction approximation (TSDIA). This scalar dissipation rate model does not assume equal length scales.

Using an asymptotic expansion of a scale parameter distinguishing the slow variation of mean flows from the fast variation of turbulent fluctuations, Yoshizawa [13] proposed the following scalar dissipation equation:

$$\frac{D\varepsilon_f}{Dt} = \varepsilon_f\left(\lambda_1\frac{1}{g}\frac{Dg}{Dt} + \lambda_2\frac{1}{\varepsilon}\frac{D\varepsilon}{Dt}\right) \tag{9}$$

As indicated by Sanders [20], this Eq. (9) leads to the analytical solution:

$$\varepsilon_f = \phi g^{\lambda_1}\varepsilon^{\lambda_2} \tag{10}$$

The value ϕ defined in Eq. (10), unfortunately is not dimensionless. The dimension of the coefficient ϕ is completely determined by the values of λ_1 and λ_2. By considering similarity behavior of the dependent variables in a round jet, the axial velocity decays with axial distance as $\widetilde{U} \sim x^{-1}$. This value is based on momentum conservation $\int_0^\infty \widetilde{U}^2 r\,\mathrm{d}r = \text{constant}$. Since the jets spread linearly, $r \sim x$ so $\widetilde{U}^2x^2 = \text{constant}$, and this gives the above scaling relations. The turbulent kinetic energy decays as $k \sim \widetilde{U}^2 \sim x^{-2}$ and the dissipation rate decays as $\varepsilon \sim k^{3/2}/l_u \sim x^{-4}$ because the integral length scale l_u increases linearly with x. When the velocity decay is known, the scalar decay can be derived based on the conservation of nozzle mass flux through each axial cross section of the jet: $\int_0^\infty \widetilde{U}\widetilde{F}r\,\mathrm{d}r = \text{constant}$. Since $r \sim x$, the scalar decays as $\widetilde{F} \sim x^{-1}$, the scalar variance decays as $\widetilde{f''^2} \sim \widetilde{F}^2 \sim x^{-2}$ and the scalar dissipation rate as $\varepsilon_f \sim x^{-4}$. Equating exponents of x in $\varepsilon_f \sim g^{\lambda_1}\varepsilon^{\lambda_2}$ and $\varepsilon_f \sim x^{-4}$, and using the scaling laws for $\widetilde{f''^2} \sim x^{-2}$ and $\varepsilon \sim x^{-4}$ this leads to $\lambda_1 + 2\lambda_2 = 2$.

Using $\lambda_1 = 1$ and $\lambda_2 = 0.5$, the coefficient ϕ should have the dimension of $\nu^{-1/2}$, and its unity is thus $\mathrm{m}^{-1}\cdot\mathrm{s}^{1/2}$. The value of the coefficient ϕ used in this study is $\phi = 7\,\mathrm{m}^{-1}\cdot\mathrm{s}^{1/2}$ and has been determined by the calibration of model predictions with experimental data. A very important feature of Eq. (10) is the absence of the turbulent kinetic energy k, compared with the equal-scale version (Eq. (8)).

2.4. Scalar dissipation rate equation

Various transport equation models for ε_f are given in the literature (Schiestel [5]). These models differ from each other by the addition of supplementary terms (Shih et al. [11], Mantel and Borghi [12]) or by changing the value of the model constants (Ruffin et al. [21], Sanders et al. [14]). In this study, we use the model developed by Mantel and Borghi [12] by applying an order of magnitude analysis. This model is Reynolds number dependent and is aimed for modelling turbulent combustion with in the flamelet concept.

Table 3
Coefficients in the scalar dissipation rate equation of Mantel and Borghi [12]

C_{P1}	C_{P2}	C_{D1}	C_{D2}
1	1	0.9	0.625

The parabolized conservation equation of ε_f in cylindrical coordinates may be written in the following general form:

$$\begin{aligned}\frac{\partial\bar\rho\widetilde{U}\varepsilon_f}{\partial x} + \frac{1}{r}\frac{\partial(r\bar\rho\widetilde{V}\varepsilon_f)}{\partial r} &= \frac{1}{r}\frac{\partial}{\partial r}\left(r\bar\rho D_f\frac{\partial\varepsilon_f}{\partial r}\right) + C_{P1}\frac{\varepsilon}{k}P_f + C_{P2}\frac{\varepsilon_f}{k}P_k \\ &\quad + C_{D1}Re_t^{1/2}\bar\rho\frac{\varepsilon}{k}\varepsilon_f - C_{D2}Re_t^{1/2}\bar\rho\frac{\varepsilon_f^2}{g}\end{aligned} \tag{11}$$

where $Re_t = k^2/(\varepsilon\nu)$ the turbulent Reynolds number, $D_f = C_f\frac{k}{\varepsilon}\widetilde{\nu''\nu''}$ (with $C_f = 0.18$) is the diffusion coefficient, $P_k = -\bar\rho\widetilde{u''\nu''}(\partial\widetilde{U}/\partial r)$ is the production term of the turbulent kinetic energy, $P_f = -2\bar\rho\widetilde{u''f''}(\partial\widetilde{F}/\partial r)$ is the production term of the scalar fluctuation, $C_{D1}Re_t^{1/2}\bar\rho\frac{\varepsilon}{k}\varepsilon_f$ is the production term by eddy stretching of scalar field by the small scales of turbulence and $C_{D2}Re_t^{1/2}\bar\rho\frac{\varepsilon_f^2}{g}$ is the destruction term by the curvature of the level surfaces having a constant value of the scalar. The coefficients of this model are listed in Table 3.

3. Numerical approach

The equations for the mean velocity, the mean mass fraction, and the velocity and scalar turbulence models are solved using a parabolic finite volume code. No transformation of the radial direction is employed. This means that the grid expands in the radial direction following the jet expansion. The computations are performed up to an axial distance of approximately $100D$ with an axial forward step size of 0.01 times the local jet half width and 80 grid points in the radial direction are used. This was sufficient to obtain a grid independent numerical solution. No boundary conditions are prescribed due to the parabolic nature of the flow. The computation progresses from section to section, and its implementation requires only the profiles at the jet nozzle.

The boundary conditions at the nozzle exit are those of a fully developed pipe flow (Laufer [22]). The mixture fraction at the inlet is equal to 1. The radial velocity, the scalar variance and their dissipation are zero at the nozzle and in the ambient. All variables at the radial jet boundary are equal

to those in the ambient. For the turbulence quantities this implies a value of zero or a negligibly small value and the energy dissipation is estimated by $\varepsilon = C_\mu k^{3/2}/0.03D$ (with $C_\mu = 0.09$).

The influence of the emission conditions on the evolution of the dynamic and scalar fields has been investigated by the authors in previous studies (Gazzah [23] and Gazzah and Sassi [24]). It proves that the emission conditions have a notable influence only in the near exit region.

4. Results and discussions

The experimental configuration of Schefer and Dibble [3] is retained for this study to permit validation. The propane/air jet issued from a round nozzle with an external diameter D_{ex} of 0.90 cm and an internal diameter D of 0.526 cm. The outlet velocity of the propane jet is set to $U_j = 53$ m·s^{-1} and that of the co-flowing air stream is $U_{\text{co}} = 9.2$ m·s^{-1}, which gives a ratio of co-flow air to jet velocity of 0.174 with a corresponding density ratio of $S_\rho = \rho_j/\rho_{\text{co}} = 1.52$. The jet Reynolds number is defined as $Re = U_j D/\nu$, and is of the order of 68 000. In the following, predictions of the far field behavior of quantities such as the scalar decay constant, the half-width of the jet, the scalar fluctuation intensity (called unmixedness) and the time scale ratio are presented and discussed.

The axial profile of the mean mixture fraction on the jet centerline $\widetilde{F}_c$ versus the normalized distance from the virtual origin $(x - x_{01})/D_e$ is shown on Fig. 1. The effective diameter is defined as $D_e = S_\rho^{-1/2} D$. It appears that the three models have no influence on the mean mixture fraction $\widetilde{F}$ and lead to the same prediction. The computed results agree well with the experimental data of Schefer and Dibble [3]. The discrepancy between the computed and measured results is less than 10%. This discrepancy is probably due to an under-estimation of the experimental values which is caused by a precession centerline jet motion. This instability enhances the mixture and leads to reduce the mean value of the scalar on the centerline.

The mixture fraction decay constant K_f defined by $1/\widetilde{F}_c = K_f(x - x_{01})/D_e$ is one of the most important characteristic of mixing jet studies. Its value is independent of x if buoyancy effects are absent, Gazzah et al. [25]. In Table 4, the predicted and the experimental values of the mixture fraction decay constant K_f are shown. A value of $K_f = 0.156$ is found. This value is very close to those obtained by Gazzah et al. [4] ($K_f = 0.154$) with a first order model. The experimental study of Schefer and Dibble [3] shows $K_f = 0.185$.

The jet spreading rate can be determined from the mean mixture fraction profiles and defined as the radial location at which the mixture fraction is equal to half its value at the centerline. Fig. 2 compares the computed and experimental jet spreading rate of the scalar field. It proves that the different models give the same prediction of the half-width L_f.

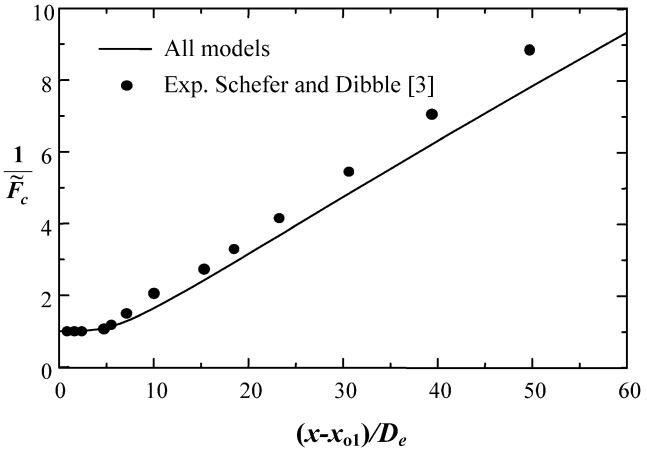

Fig. 1. Centerline values of the mixture fraction.

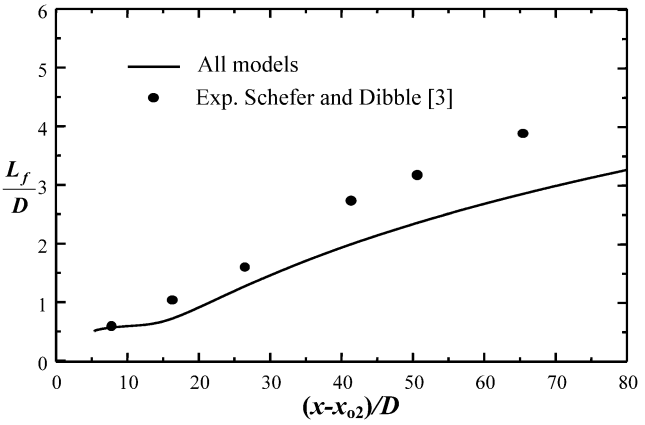

Fig. 2. Centerline values of the mixture fraction half-width.

The computed L_f has the same behavior as the measured quantity. The difference observed is probably due to the precession centerline motion as well as the intermittence in the two mixing layers. This mechanism leads to an over-estimation of the measured half-width. It should be noted that when there is no co-flow, the computed half-width agrees much better with the experimental data (Gazzah et al. [4]).

The scalar half-width can be written as

$$\frac{L_f}{D} = S_f^{1/2} \frac{(x - x_{02})}{D} \tag{12}$$

where $S_f^{1/2}$ is the scalar spreading rate. In presence of co-flow, the half-width is no longer a linear function of x, and $S_f^{1/2}$ cannot be easily determined. Therefore $S_f^{1/2}$ depends on the axial distance and is not a useful concept in a co-flowing jet. The estimated spreading rate $S_f^{1/2} = 0.043$ is smaller than that obtained by Schefer and Dibble [3] $S_f^{1/2} = 0.06$, with the same value of co-flow and the value ($S_f^{1/2} = 0.086$) obtained by Dyer [26] in a propane-air jet using a different value of the co-flow. The values of half-width and spreading rate are affected by the co-flowing air.

Table 4
Model predictions for asymptotic values of mixture fraction decay, the spreading rate, the unmixedness and the time scale ratio at various models

Models	U_{co}/U_j	K_f	$S_f^{1/2}$	$\sqrt{g_{max}}/\sqrt{g_c}$	r_{max}/L_f	$\sqrt{g_c}/F_c$	R_τ
RSM equal	0.174	0.156	0.043	1.13	0.70	0.26	2.00
RSM non-equal	0.174	0.156	0.043	1.14	0.76	0.27	2.08
Mantel and Borghi [12]	0.174	0.156	0.043	1.07	0.70	0.34	1.51
Mantel and Borghi modified	0.174	0.156	0.043	1.10	0.70	0.29	1.92
k–ε (Gazzah et al. [4])	0.174	0.154	0.045	1.16	0.75	0.26	2.00
Exp. Schefer and Dibble [3]	0.174	0.185	0.06	1.24	0.96	0.265	–
Dyer [26]	0.026	0.18	0.086	1.29	0.8	0.15	–
Djeridane [27] $S_\rho = 0.94$	0.10	0.151	0.052	1.22	0.85	0.19	–
Panchapakesan and Lumley [7] $S_\rho = 0.14$	0.00	0.27	0.13	1.27	0.61	0.22	1.5

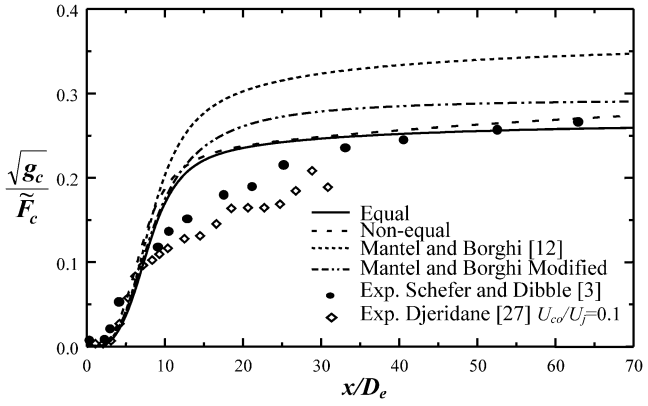

Fig. 3. Centerline values of the scalar fluctuation intensity.

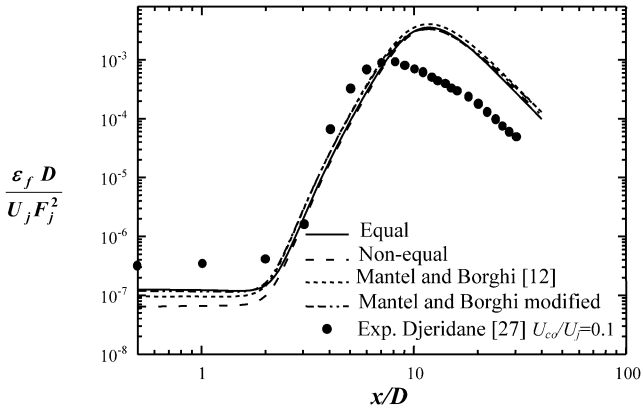

Fig. 4. Centerline values of ε_f predicted with the different models.

The axial profile of the scalar fluctuation intensity on the jet centerline is shown on Fig. 3. The different profiles have similar behavior. They increase with x and then they reach an asymptotic value. The asymptotic value $\sqrt{g_c}/\widetilde{F}_c$ obtained by each model as well as the experimental asymptotic value obtained by Schefer and Dibble [3] and by Djeridane [27] are listed in Table 4.

The equal and non-equal scales models give rise respectively to an asymptotic value of 0.26 and 0.27 at $x/D_e > 20$. These values are both very close to experimental data. However, it appears that results obtained using Mantel and Borghi model differ from that obtained using the two other models. To improve the prediction of the asymptotic value obtained with Mantel and Borghi model, the constant involved in the destruction term is modified. When a value of $C_{D2} = 0.5$ is used, the so-called modified Mantel and Borghi model leads to a result in good agreement with the experimental data.

Using a ratio of co-flow to jet velocity $U_{co}/U_j = 0.1$, Djeridane [27] obtained an asymptotic value of the scalar fluctuation intensity of 19%. This value is smaller than that obtained by Schefer and Dibble [3]. As pointed out by Djeridane [27], this difference is due to the fact that the two experiments have not the same co-flow and the asymptotic value increases when the ratio U_{co}/U_j increases.

Since several models have been adopted to predict the scalar dissipation rate ε_f, we obtained different estimations of the scalar fluctuation intensity (Fig. 3) because ε_f is involved in the destruction terms of the scalar variance $\tilde{f}''^2$.

It is rightful to ask how ε_f or $\tilde{f}''^2$ will affect the mean and the turbulent quantities. As shown in Table 1, $\tilde{f}''^2$ appears explicitly in the buoyancy term in the equation of $\widetilde{u''f''}$. It is well known (Gazzah et al. [25]), that the contribution of the buoyancy term is negligible in the near region. Therefore, the estimate of ε_f affects only the scalar variance $\tilde{f}''^2$ and it has no affect on the mean quantities (Figs. 1, 2, 5).

Fig. 4 shows the axial profiles of the computed scalar dissipation rate obtained with several models. It appears that the different profiles have similar behaviors. The results obtained with Mantel and Borghi are greater than the prediction of the other models. This is expected and compatible with the prediction of the scalar fluctuation intensity. Fig. 4 shows that the scalar dissipation rate predicted with all models exhibits an increase with increasing the axial distance before attaining a maximum and then it decreases for large distance from the exit. This is in good agreement with the air/air jet behavior was obtained by Djeridane [27]. The difference between the values of the measured and computed scalar dissipation rate is mainly due to the difference of the values of the co-flow ratio. The experiments of Djeridane [27] are carried out with a co-flow ratio smaller than the ratio used in the present study. Indeed, if the computation is made with a co-flow ratio equal to that relative to experimental data of Djeridane [27] (Fig. 4), the agreement between the computed and experimental results becomes better.

In Figs. 5 and 6, the radial profiles of the mixture fraction and the scalar fluctuation intensity normalized by their re-

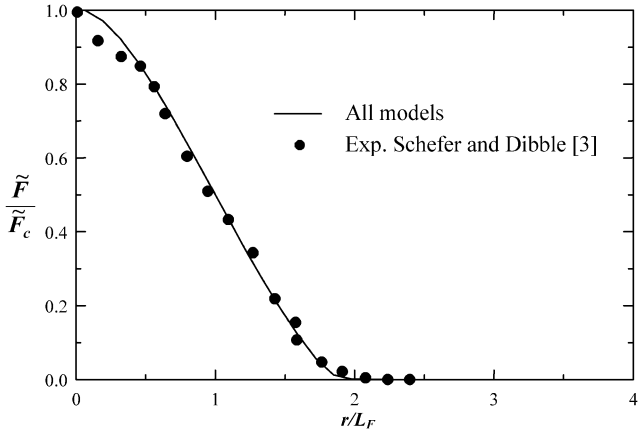

Fig. 5. Mixture fraction radial profiles predicted at $x/D = 30$.

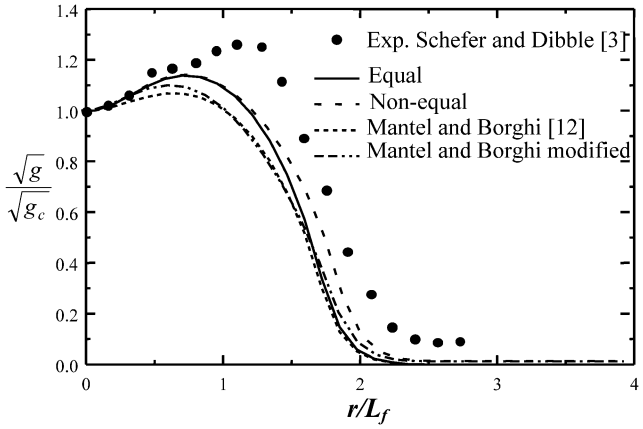

Fig. 6. Scalar fluctuation intensity radial profiles predicted with the different models at $x/D = 30$.

spective centerline values versus the radial distance normalized by L_F are plotted. The predicted profiles are compared with the measurements of Schefer and Dibble [3] for the downstream section $x/D = 30$. As expected, in this region the computation gives the affinity of the profiles and an evolution alike of that related to a simple jet is found. We notice that all models are in good agreement with the experimental data of Schefer and Dibble [3] for the radial profiles of the mixture fraction. However, concerning the radial scalar fluctuation intensity profiles (Fig. 6) the agreement is acceptable in the sense that all models show similar behavior to the experimental one. Besides to than the experimental uncertainties and the influence of the emission conditions on the prediction of the jet structure, the observed differences could be due to a limitation effect of the parabolic approach, and to the influence of intermittence which is not explicitly taken into account in this model. However, it is noted that none of the models predicts the weak local off-axis maximum in the experimental curves. A comparison of the maximum fluctuations $\sqrt{g_{\max}}/\sqrt{g_c}$ (unmixedness) and their radial locations $r_{\max}/L_F$ is also shown in Table 4.

Fig. 7 exhibits the radial profile of the computed time scale ratio R_τ obtained using different models. In the central

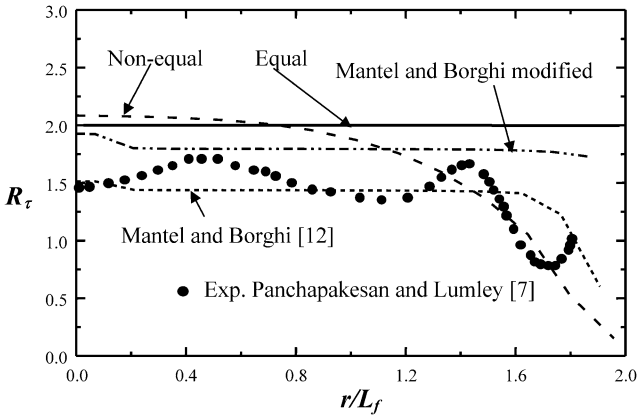

Fig. 7. Time scale ratio R_τ radial profiles predicted by the different models at $x/D = 30$.

region, R_τ is almost constant whereas in the outer region R_τ decreases significantly. The measurements in the Helium-air jet of Panchapakesan and Lumley [7] of R_τ show a similar trend. The quantitative values predicted by the present models and Panchapakesan and Lumley [7] are different, but unfortunately there are no measurements of R_τ available in propane jet with co-flowing air. The difference between the results obtained by the modified Mantel and Borghi model and the experimental data is mainly due to the fact the composition of the mixture is not the same. Indeed, if the computation is made for Helium-air jet, the agreement between experimental and computed results is improved. Therefore, the experimental results are displayed only for qualitative comparison. The modified Mantel and Borghi model behaves like the equal scale model. The predicted asymptotic centerline values of R_τ, using different models, are shown in Table 4.

5. Conclusion

The turbulent transport of scalar fluctuation has been investigated using several models: the equal scales, the non-equal scales and the transport equation models within the framework of the second order turbulence closure model. The influence of these models on the scalar mixture fraction, the unmixedness, the half-width of the jet and the time scale ratio have been examined. The obtained results showed a good qualitative agreement with data from experiments of Schefer and Dibble [3] for a propane turbulent jet into a co-flowing air stream.

The standard Mantel and Borghi [12] model does not predict convenably the asymptotic value of turbulent scalar intensity. To improve this prediction we modified the destruction terms constants. Although its simplicity, the algebraic non-equal scales model provides satisfactory results. Furthermore, the dynamic and scalar time scale ratio appears to depend on the jet radial distance as it has been observed experimentally. The algebraic non-equal scales model seem to

be promising since it is able to predict accurately the scalar field.

In the near future, we intend to use the different models to investigate a reacting flow such as a turbulent diffusion flame.

References

[1] J.L. Borean, D. Huilier, H. Burnage, On the effect of a co-flowing stream on the structure of an axisymmetric turbulent jet, Experimental Thermal Fluid Sci. 17 (1998) 10–17.

[2] Y. Antoine, F. Lemoine, M. Lebouché, Turbulent transport of a passive scalar in a round jet discharging into a co-flowing stream, European J. Mech. B Fluids 20 (2001) 275–301.

[3] R.W. Schefer, R.W. Dibble, Mixture fraction field in a turbulent non-reacting propane jet, AIAA J. 39 (1) (2001) 64–72.

[4] M.H. Gazzah, H. Belmabrouk, M. Sassi, A numerical study of the scalar field in turbulent round jet with co-flowing stream, Comput. Mech. 34 (5) (2004) 430–437.

[5] R. Schiestel, Modélisation et simulation des écoulements turbulents, Hermès, Paris, 1993.

[6] E. Ruffin, Etude de jets turbulents à densité variable à l'aide de modèles de transport au second ordre, Thèse de doctorat, université d'Aix-Marseille II, 1994.

[7] N.R. Panchapakesan, J.L. Lumley, Turbulence measurements in axisymmetric jets of air and helium, Part 2. Helium jet, J. Fluid Mech. 246 (1993) 225–247.

[8] R.W. Dibble, W. Kollmann, M. Farshchi, R.W. Schefer, Second-order closure for turbulent non-premixed flames: scalar dissipation and heat release effects, in: 21st Symposium (International) on Combustion, 1986, pp. 1329–1340.

[9] J.F. Lucas, Analyse du champ scalaire au sein d'un jet turbulent axisymétrique à densité variable, Thèse, Aix-Marseille II, 1998.

[10] L. Pietri, M. Amielh, F. Anselmet, Simultaneous measurements of temperature and velocity fluctuations in a highly heated jet combining a cold wire and laser Doppler anemometry, Internat. J. Heat Fluid Flow 21 (2000) 22–36.

[11] T.H. Shih, J.L. Lumley, J. Janicka, Second-order modelling of variable-density mixing layer, J. Fluid Mech. 180 (1987) 93–116.

[12] Th. Mantel, R. Borghi, A new model of turbulent wrinkled flame propagation based on a scalar dissipation equation, Combust. Flame 96 (1994) 443–457.

[13] A. Yoshizawa, Statistical modelling of passive-scalar diffusion in turbulent shear flows, J. Fluid Mech. 195 (1988) 541–555.

[14] J.P. Sanders, B. Sarh, I. Gökalp, Variable density effects in axisymmetric isothermal turbulent jets: A comparison between a first- and a second-order turbulence model, Internat. J. Heat Mass Transfer 40 (4) (1997) 823–842.

[15] B.E. Launder, D.B. Spalding, The numerical computation of turbulent flows, Comput. Method Appl. Mech. Engrg. 3 (1974) 269–289.

[16] S.B. Pope, An explanation of the turbulent round-jet/plane-jet anomaly, AIAA J. 16 (1978) 279–281.

[17] A. Rubel, On the vortex stretching modification of the k–ε model in radial jets, AIAA J. 23 (1985) 1129–1130.

[18] C.G. Speziale, On nonlinear k–l and k–ε models of turbulence, J. Fluid Mech. 178 (1987) 459–475.

[19] R. Borghi, D. Escudie, Assessment of a theoretical model of turbulent combustion by comparison with a simple experiment, Combust. Flame 56 (1984) 149–164.

[20] J.P.H. Sanders, A.P.G.G. Lamers, Scalar transport in turbulent jet, Internat. Comm. Heat Mass Transfer 19 (1992) 851–858.

[21] E. Ruffin, E. Schiestel, F. Anselmet, M. Amielh, L. Fulachier, Investigation of characteristic scales in variable density turbulent jets using a second-order model, Phys. Fluids 6 (1994) 2785–2799.

[22] J. Laufer, The structure of turbulence in fully developed pipe flow, National Advisory Committee for Aeronautics, Report 1174, 1953.

[23] M.H. Gazzah, Contribution à l'étude d'un jet turbulent à masse volumique variable, Thèse de doctorat, Ecole Nationale d'Ingénieurs de Monastir, Tunisie, 2002.

[24] M.H. Gazzah, M. Sassi, Etude numérique de l'influence des conditions opératoires sur le développement d'un jet turbulent à densité variable, Rev. Méc. Appl. Théorique 1 (5) (2003) 311–321.

[25] M.H. Gazzah, M. Sassi, B. Sarh, I. Gökalp, Simulation numérique des jets turbulent subsoniques à masse volumique variable par le modèle k–ε, Internat. J. Thermal Sci. 41 (1) (2002) 51–62.

[26] T.M. Dyer, Rayleigh scattering measurements of time-resolved concentration in a turbulent propane jet, AIAA J. 17 (1979) 912–914.

[27] T. Djeridane, Contribution à l'étude expérimentale de jets turbulents axisymétriques à densité variable, Thèse de Doctorat, Université d'Aix-Marseille II, 1994.